

Modeling of Quantum Cascade Lasers by nonequilibrium Green's functions

A. Wacker, M. Lindskog, and D.O. Winge

Mathematical Physics, Lund University, Box 118, 22100 Lund, Sweden

e-mail: Andreas.Wacker@fysik.lu.se

INTRODUCTION

The quantum cascade laser (QCL) [1] has become an important device for IR radiation allowing a large variety of spectroscopic applications [2]. QCLs are based on optical transitions between electronic subbands in semiconductor heterostructures. Here the choice of the layer structure allows to specify the separation of the upper and lower laser level, and lasers covering two decades of the optical spectrum have been realized. A central feature is that the inversion is obtained by the specific current flow in biased structures. Thus the operation is based on an intriguing interplay between tunneling and scattering transitions which requires a quantum treatment. Over the last decade our group has developed a simulation package based on nonequilibrium Green's functions which allows for a quantitative modeling[3]. In this talk, this package is presented in detail.

SET-UP OF THE SCHEME

We consider a semiconductor heterostructure, which has a period d in growth direction (along the z axis), such as a superlattice or a QCL. We use a basis $\Psi_{\nu n, \mathbf{k}}(x, y, z) \propto \varphi_{\nu}(z - nd)e^{i(k_x x + k_y y)}$, where the wavefunctions $\varphi_{\nu}(z - nd)$ are orthonormal for different combinations of their indices (n, ν) . Typically, we take into account three $(n = -1, 0, 1)$ periods for QCLs, but more periods are required for superlattices. The Hamiltonian of the perfect structure (including the mean field and the oscillating field in the cavity) is diagonal in \mathbf{k} and is fully taken into account. Scattering is treated perturbatively by self-energies, which become matrices $\Sigma_{\nu\nu', n'n'}(\mathbf{k}; t_1, t_2)$ with respect to the basis states applied. For given self-energies, we solve the Dyson equation and the Keldysh relation to obtain

the Green's function $G_{\nu\nu', n'n'}(\mathbf{k}; t_1, t_2)$. With these Green's functions the self-energies are evaluated around the central period $n = 0$, where finite size effects are least. Applying periodic boundary conditions the full self-energy matrix is generated. This procedure is repeated, until convergence is reached, see Fig. 1.

Currently, the following scattering processes are included: Polar scattering for optical phonons, deformation potential for acoustic phonons, interface roughness, ionized impurity scattering, and alloy scattering following standard procedures. As a major approximation the scattering matrix elements are replaced by averaged values for typical k values of the initial and final state. This provides k -independent self-energies, which strongly reduces the memory requirements.

BENEFITS FROM THE MODEL

The Green's functions provide full information for the system based on a fully consistent microscopic quantum kinetic approach. Thus all relevant quantities such as the current density and the gain spectrum can be evaluated based on nominal sample parameters. For most samples we find quantitative agreement for the current with experiment within 20%, see e.g. Fig. 2. Furthermore, we can extract the energetical distribution of carriers and currents, which, e.g., allows to identify leakage paths. An example is given in Fig. 3.

REFERENCES

- [1] J. Faist *et al.*, Science **264**, 553 (1994).
- [2] R. F. Curl *et al.*, Chem. Phys. Lett. **487**, 1 (2010).
- [3] A. Wacker, M. Lindskog, and D. Winge, IEEE Journal of Selected Topics in Quantum Electronics **19**, 1200611 (2013).
- [4] E. Dupont *et al.*, Journal of Applied Physics **111**, 73111 (2012).

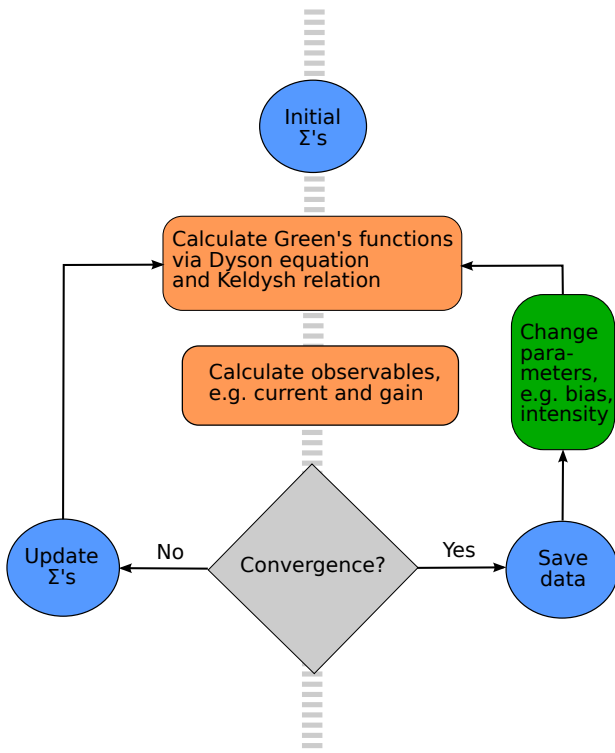


Fig. 1. Flowchart of our simulations scheme

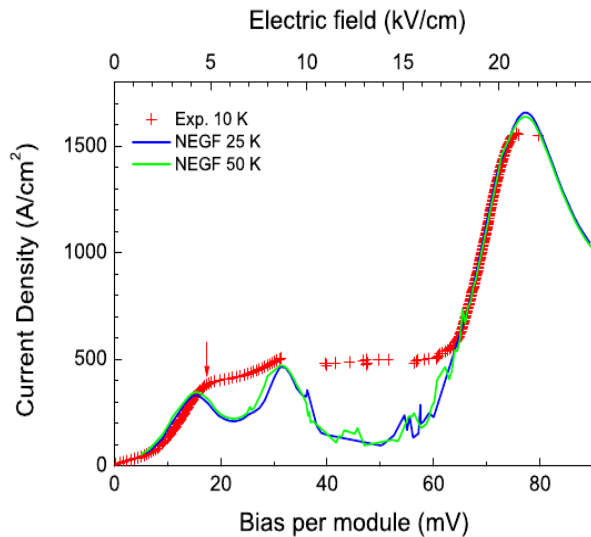


Fig. 2. Calculated current-bias characteristic together with experimental data for a THz-QCL. The simulation correctly reproduces all current peaks. Between the peaks the experimental current differs. This is most likely due to domain formation, which is not included in the simulation. From [4]

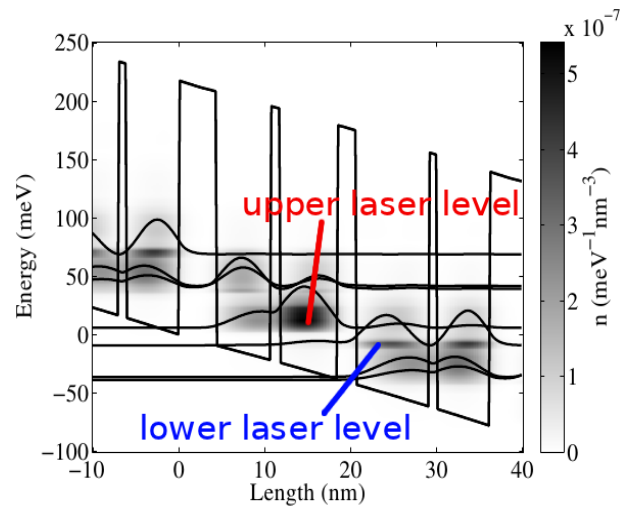


Fig. 3. Energetically resolved carrier density at the current peak of Fig. 2. One observes carrier accumulation before the thick barrier. A thinner barrier would allow for a higher population of the upper laser, from [4].